

Matter fields in triangle–hinge models

Masafumi Fukuma^{1,*}, Sotaro Sugishita^{1,2,*}, and Naoya Umeda^{1,*}

¹*Department of Physics, Kyoto University, Kyoto 606-8502, Japan*

²*Present address: Department of Physics, Osaka University, Toyonaka 560-0043, Japan*

*E-mail: fukuma@gauge.scphys.kyoto-u.ac.jp, sugishita@het.phys.sci.osaka-u.ac.jp,
 n_umeda@gauge.scphys.kyoto-u.ac.jp

Received March 7, 2016; Accepted April 4, 2016; Published May 24, 2016

.....
 The worldvolume theory of membranes is mathematically equivalent to 3D quantum gravity coupled to matter fields corresponding to the target space coordinates of an embedded membrane. In a recent paper [M. Fukuma et al., J. High Energy Phys. **1507**, 088 (2015) [arXiv:1503.08812 [hep-th]]], a new class of models that generate 3D random volumes was introduced, where the Boltzmann weight of each configuration is given by the product of values assigned to the triangles and the hinges. These *triangle–hinge models* describe 3D pure gravity and are characterized by semisimple associative algebras. In this paper, we introduce matter degrees of freedom to the models by coloring simplices in such a way that they have local interactions. This is achieved simply by extending the associative algebras of the original triangle–hinge models, and the profile of the matter field is specified by the set of colors and the form of the interactions. The dynamics of a membrane in D -dimensional spacetime can then be described by taking the set of colors to be \mathbb{R}^D . By taking another set of colors, we can also realize 3D quantum gravity coupled to various spin models such as the Ising model. 3D colored tensor models can also be realized as triangle–hinge models by coloring tetrahedra, triangles, and edges at one time.

Subject Index B25, B83, B86, E05

1. Introduction

M-theory is a candidate for the theory of everything including quantum gravity, where membranes are believed to be fundamental objects [2–6]. The worldvolume theory of membranes is mathematically equivalent to 3D quantum gravity coupled to matter fields, corresponding to the target space coordinates of an embedded membrane [7]. However, our understanding of 3D quantum gravity coupled to matter is still not at a sufficient level if we compare it with the 2D case, where the dynamics of random surfaces has been well understood from various perspectives by using matrix models as an analytic tool (see, e.g., Ref. [8] for a review). In fact, matrix models generate random surfaces as Feynman diagrams and can be solved analytically. This solvability enables us to find a critical point around which the continuum limit is taken, and we now have a clear understanding of 2D quantum gravity coupled to a large class of matter fields (e.g., $c \leq 1$ noncritical string theories). Thus, we expect that our understanding of the dynamics of membranes will be substantially developed if we can find a 3D analog of matrix models that generates 3D random volumes as Feynman diagrams and allows us to investigate the dynamics analytically (hopefully at the level of matrix models). It will then lead to a consistent formulation of M-theory if such models admit the introduction of supersymmetry and do not have an issue like the $c = 1$ barrier in 2D theories.

Recently, as a first step in this direction, the authors constructed a new class of models that generate 3D random volumes [1]. Since the dynamical variables are given by matrices and each model can be specified by a semisimple associative algebra, these models have the potential to be solved analytically using matrix model techniques. We call these models *triangle–hinge models* because each Feynman diagram is treated as consisting of “triangles and hinges.”¹ This is in sharp contrast to the setup in tensor models [10–12] or in group field theory [13,14], where the minimum unit of the Feynman diagram is given by a tetrahedron.² Triangle–hinge models have an intrinsic problem that 3D volumes cannot be assigned to a large portion of Feynman diagrams. However, one can reduce the set of possible diagrams such that they represent only and all of the tetrahedral decompositions of 3D manifolds, by introducing specific interaction terms and taking an appropriate limit of parameters in the models [1]. Therefore, triangle–hinge models can be regarded as discrete models of 3D quantum gravity.

The original triangle–hinge models given in Ref. [1] do not have any extra degrees of freedom other than those of simplicial decompositions and thus describe 3D *pure* gravity. However, in order to describe the dynamics of membranes, we need to extend the models so that they contain matter fields corresponding to the target space coordinates.

The main aim of this paper is to introduce local matter degrees of freedom to triangle–hinge models, by coloring simplices in tetrahedral decompositions (actually simplices of arbitrary dimensions (tetrahedra, triangles, edges, and vertices)). The coloring is realized within the algebraic framework of the original triangle–hinge models, and we only need to extend the defining semisimple associative algebras and to modify the interaction terms accordingly. The matter fields thus obtained have local interactions because colored simplices interact only with their neighbors.

A matter field is specified by the set of colors and the form of interactions. The worldvolume theory of membranes is given by taking the set of colors to be \mathbb{R}^D with a local interaction in the target spacetime. Besides this, we can construct various spin systems on random volumes. For example, the Ising model on random volumes can be realized by taking the set of colors to be $\mathbb{Z}_2 = \{+, -\}$ and by assigning a color (\pm) to each tetrahedron. We can also set up q -state Potts models, restricted solid-on-solid (RSOS) models [26], and even more generic models on random volumes. We will further show that 3D colored tensor models [27]³ can be realized as triangle–hinge models by assigning specific matter degrees of freedom to tetrahedra, triangles, and edges at one time.

This paper is organized as follows. In Sect. 2, we review the basic structure of triangle–hinge models. In Sect. 3, we give a general prescription to introduce matter degrees of freedom to the models. In Sect. 4, we review the Feynman rules of colored tensor models and show that they can be reproduced from triangle–hinge models by coloring tetrahedra, triangles, and edges in a specific way. Section 5 is devoted to the conclusion.

¹ A similar approach was taken for 3D topological lattice field theories [9].

² There is another type of tensor model (called the canonical tensor model) that realizes the constraints in the canonical quantization of gravity [15–20]. An interesting connection to the random tensor network is studied in Refs. [21–25].

³ Although the original tensor models can generate diagrams not homeomorphic to pseudomanifolds, colored tensor models are free from this issue [28]. Furthermore, it is known that colored tensor models have good analytical properties (see, e.g., Ref. [29] for a review).

2. Review of triangle–hinge models

In this section, we give a brief review of triangle–hinge models, which generate random diagrams consisting of triangles glued together along multiple hinges (see the original paper [1] for details). Note that a tetrahedral decomposition can always be regarded as a Feynman diagram of a triangle–hinge model, as can be understood from Fig. 1.

2.1. Generalities

We first give the definition of triangle–hinge models. The dynamical variables are given by $N \times N$ real symmetric matrices A and B :

$$A_{ij} = A_{ji}, \quad B^{ij} = B^{ji} \quad (i, j = 1, \dots, N), \quad (2.1)$$

and the action takes the form

$$S[A, B] = \frac{1}{2} A_{ij} B^{ij} - \frac{\lambda}{6} C^{ijklmn} A_{ij} A_{kl} A_{mn} - \sum_{k \geq 2} \frac{\mu_k}{2k} B^{i_1 j_1} \dots B^{i_k j_k} y_{i_1, \dots, i_k} y_{j_k, \dots, j_1}, \quad (2.2)$$

where C^{ijklmn} , y_{i_1, \dots, i_k} , λ , and μ_k are real-valued coupling constants. The Feynman diagrams are obtained by expanding the action (2.2) around the “kinetic term” $(1/2)A_{ij}B^{ij}$. The interaction vertices corresponding to $\lambda C^{i_1 j_1 i_2 j_2 i_3 j_3}$ and $\mu_k y_{i_1, \dots, i_k} y_{j_k, \dots, j_1}$ can be represented by triangles and k -hinges, respectively, as in Fig. 2, if we assume the coupling constants to have the following symmetry properties:

$$C^{i_1 j_1 i_2 j_2 i_3 j_3} = C^{i_2 j_2 i_3 j_3 i_1 j_1}, \quad C^{i_1 j_1 i_2 j_2 i_3 j_3} = C^{j_3 i_3 j_2 i_2 j_1 i_1}, \quad (2.3)$$

$$y_{i_1 i_2, \dots, i_k} = y_{i_2, \dots, i_k i_1}, \quad (2.4)$$

which realize the symmetries of triangles and hinges under rotations and flips.⁴ The propagator has the form

$$\langle A_{ij} B^{kl} \rangle = \delta_i^k \delta_j^l + \delta_i^l \delta_j^k, \quad (2.5)$$

where the two terms on the right-hand side correspond to two ways of gluing an edge of a triangle to that of a hinge (in the same or opposite direction). Thus, the action (2.2) gives Feynman diagrams consisting of triangles that are glued together along multiple hinges in all possible ways.

A wide class of triangle–hinge models can be defined by semisimple associative algebras \mathcal{A} of linear dimension N [1]. With a basis $\{e_i\}$ ($i = 1, \dots, N$) of \mathcal{A} [$\mathcal{A} = \bigoplus_{i=1}^N \mathbb{R}e_i$], the multiplication

⁴ In fact, when multiplied by $A_{i_1 j_1} A_{i_2 j_2} A_{i_3 j_3}$ ($A_{ij} = A_{ji}$), only such parts of $C^{i_1 j_1 i_2 j_2 i_3 j_3}$ survive that are invariant under interchanges of indices i_α and j_α ($\alpha = 1, \dots, 3$) and under permutations of three pairs of indices $(i_1 j_1)$, $(i_2 j_2)$, and $(i_3 j_3)$. Thus, one could assume the symmetry $C^{i_1 j_1 i_2 j_2 i_3 j_3} = C^{j_1 i_1 i_2 j_2 i_3 j_3} = C^{i_2 j_2 i_1 j_1 i_3 j_3}$ in the action (2.2). We, however, do not assume this symmetry and regard the contributions from $C^{i_1 j_1 i_2 j_2 i_3 j_3}$, $C^{j_1 i_1 i_2 j_2 i_3 j_3}$, and $C^{i_2 j_2 i_1 j_1 i_3 j_3}$ as giving different Feynman diagrams. This prescription enables us to interpret the interaction vertices as triangles and is commonly adopted in the standard treatment of matrix models. Note that only the fully symmetric part is actually left when all the diagrams are summed. The same argument is applied to the hinge parts.

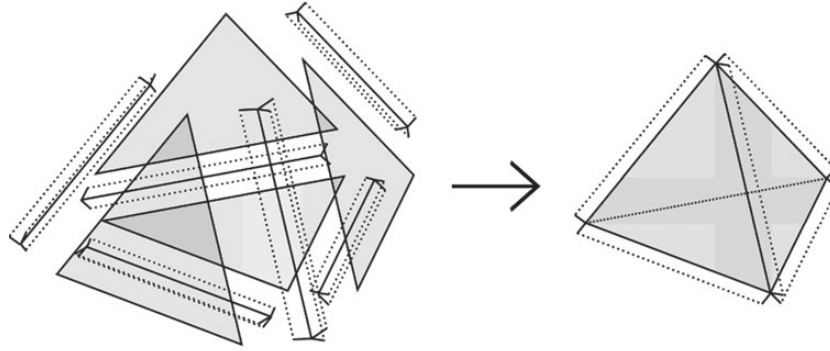


Fig. 1. Construction of tetrahedral decompositions with triangles and multiple hinges [1].

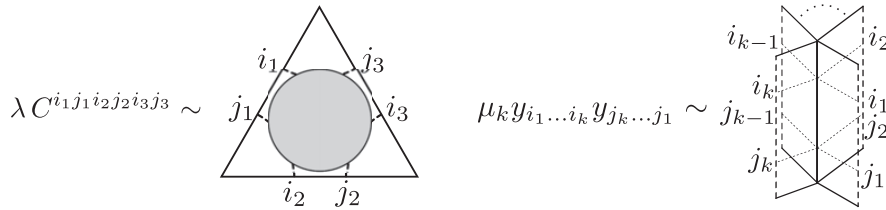


Fig. 2. Triangles and multiple hinges [1].

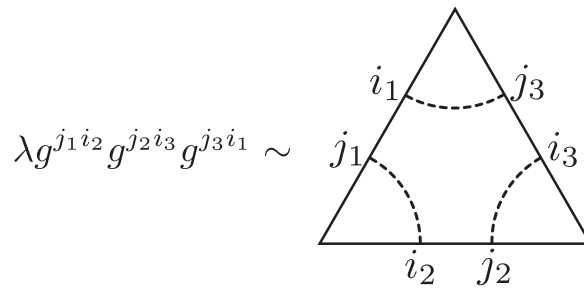


Fig. 3. Index lines on a triangle [1].

is expressed as

$$e_i \times e_j = y_{ij}^k e_k. \tag{2.6}$$

Then, the cyclically symmetric rank- k tensor y_{i_1, \dots, i_k} is constructed from the structure constants y_{ij}^k as

$$y_{i_1, \dots, i_k} \equiv y_{i_1 j_1}^{j_k} y_{i_2 j_2}^{j_1} \cdots y_{i_k j_k}^{j_{k-1}}. \tag{2.7}$$

The rank-two tensor y_{ij} is especially denoted by g_{ij} and is called a metric, $g_{ij} \equiv y_{ij} = y_{ik}^\ell y_{j\ell}^k$.⁵ A possible choice of C^{ijklmn} satisfying (2.3) is

$$C^{ijklmn} = g^{jk} g^{lm} g^{ni}, \tag{2.8}$$

which corresponds to the index lines illustrated in Fig. 3. This is not the unique solution to the condition (2.3), and we will use this arbitrariness later (see (2.18)).

⁵ An associative algebra \mathcal{A} is semisimple (i.e., a direct sum of matrix rings) if and only if the metric $g = (g_{ij})$ has its inverse $g^{-1} \equiv (g^{ij})$ [30].

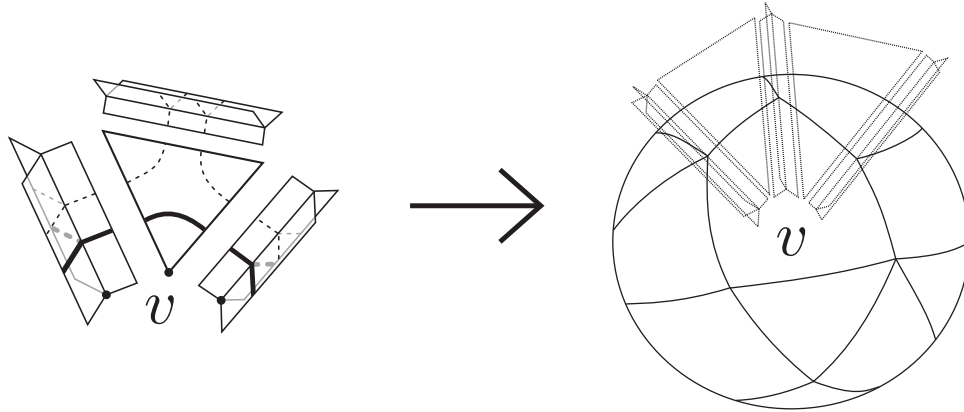


Fig. 4. Part of an index network (left) and a connected index network around a vertex v (right) [1]. When hinges share a common vertex v , their index lines are connected via intermediate triangles and give a polygonal decomposition of a closed surface enclosing vertex v . The closed surface need not be a sphere, and we denote its genus by $g(v)$.

The free energy of the model is given by the summation of Boltzmann weights $w(\gamma)$ over all possible connected diagrams γ :

$$\log Z = \sum_{\gamma} w(\gamma), \tag{2.9}$$

$$w(\gamma) = \frac{1}{S(\gamma)} \lambda^{s_2(\gamma)} \left(\prod_{k \geq 2} \mu_k^{s_1^k(\gamma)} \right) \mathcal{F}(\gamma), \tag{2.10}$$

where $S(\gamma)$ denotes the symmetry factor of diagram γ , $s_2(\gamma)$ the number of triangles, and $s_1^k(\gamma)$ the number of k -hinges. $\mathcal{F}(\gamma)$ is a function of C^{ijklmn} and y_{i_1, \dots, i_k} (and thus a function only of the structure constants y_{ij}^k) and is called the *index function of diagram γ* .

It is easy to see that the index function $\mathcal{F}(\gamma)$ is the product of the contributions $\zeta(v)$ from vertices v (to be called the *index functions of vertices*):

$$\mathcal{F}(\gamma) = \prod_{v: \text{vertex of } \gamma} \zeta(v). \tag{2.11}$$

In fact, index lines out of different hinges are connected if and only if the hinges share a common vertex in γ , and then a connected component of the index lines forms a polygonal decomposition of a closed 2D surface enclosing a vertex (see Fig. 4).⁶ Moreover, $\zeta(v)$ is a 2D topological invariant of the closed surface around v . In fact, $\zeta(v)$ is the product of y_{ij}^k whose indices are all contracted appropriately, and is invariant under 2D topology-preserving local moves that are generated by the fusion move and the bubble move (see Fig. 5), which are equivalent to the condition of associativity $y_{ij}^l y_{lk}^m = y_{jk}^l y_{il}^m$ and the definition of the metric, $y_{ik}^l y_{jl}^k = g_{ij}$, respectively [30]. Thus the index function $\zeta(v)$ is the 2D topological invariant associated with algebra \mathcal{A} [30] and is characterized only by the genus $g(v)$ of the closed surface around vertex v , $\zeta(v) = \mathcal{I}_{g(v)}[\mathcal{A}]$. Therefore, the free energy

⁶ As is argued in Ref. [1], a 2D surface can be uniquely assigned to each connected index network by carefully following the contraction of indices.

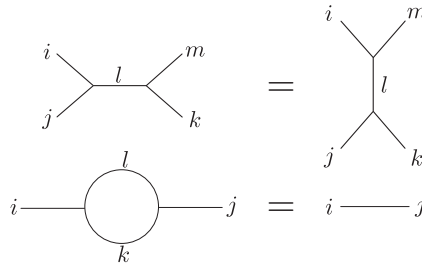


Fig. 5. Fusion move (top) and bubble move (bottom) [30]. The index function $\zeta(v)$ is invariant under these 2D topology-preserving local moves.

of the model takes the form

$$\log Z = \sum_{\gamma} \frac{1}{S(\gamma)} \lambda^{s_2(\gamma)} \left(\prod_{k \geq 2} \mu_k^{s_1^k(\gamma)} \right) \prod_{v: \text{vertex}} \mathcal{I}_g(v)[\mathcal{A}]. \tag{2.12}$$

2.2. Matrix ring

The simplest example of semisimple algebra is the matrix ring $M_n(\mathbb{R}) = \bigoplus \mathbb{R}e_{ab}$ (with linear dimension $N = n^2$). Here, we take the basis to be $\{e_{ab}\}$ ($a, b = 1, \dots, n$), where e_{ab} is a matrix unit whose (c, d) element is $(e_{ab})_{cd} = \delta_{ac}\delta_{bd}$. Note that indices i are now double indices, $i = (a, b)$. When we take $\mathcal{A} = M_n(\mathbb{R})$ as the defining associative algebra of a triangle–hinge model, the choice of (2.7) and (2.8) gives the action of the form [1]

$$S = \frac{1}{2} A_{abcd} B^{abcd} - \frac{\lambda}{6n^3} A_{bacd} A_{dcef} A_{feab} - \sum_{k \geq 2} \frac{n^2 \mu_k}{2k} B^{a_1 a_2 b_2 b_1} B^{a_2 a_3 b_3 b_2} \dots B^{a_k a_1 b_1 b_k}. \tag{2.13}$$

Here, the variables A and B satisfy

$$A_{abcd} = A_{cdab}, \quad B^{abcd} = B^{cdab}, \tag{2.14}$$

and we have used the fact that the tensor $C^{i_1 j_1 i_2 j_2 i_3 j_3} = C^{a_1 b_1 c_1 d_1 a_2 b_2 c_2 d_2 a_3 b_3 c_3 d_3}$ in (2.8) takes the form

$$C^{a_1 b_1 c_1 d_1 a_2 b_2 c_2 d_2 a_3 b_3 c_3 d_3} = \frac{1}{n^3} \delta^{d_1 a_2} \delta^{d_2 a_3} \delta^{d_3 a_1} \delta^{b_3 c_2} \delta^{b_2 c_1} \delta^{b_1 c_3}. \tag{2.15}$$

The interaction terms can then be expressed by thickened triangles as in Fig. 6. Accordingly, the index lines in Fig. 4 are drawn with double (or thickened) lines as in Fig. 7. Polygons formed by index loops will be called *index polygons*. One can show that \mathcal{I}_g in (2.12) is given by n^{2-2g} for a connected index network of genus g [1].

Furthermore, the model with $\mathcal{A} = M_n(\mathbb{R})$ has a duality that interchanges the roles of triangles and hinges [1]. In fact, with the new variables dual to A and B ,⁷

$$\tilde{A}^{abcd} \equiv A_{bcda}, \quad \tilde{B}^{abcd} \equiv B^{bcda}, \tag{2.16}$$

⁷ We will use this duality transformation when we discuss a duality of coloring in Sect. 3.4.

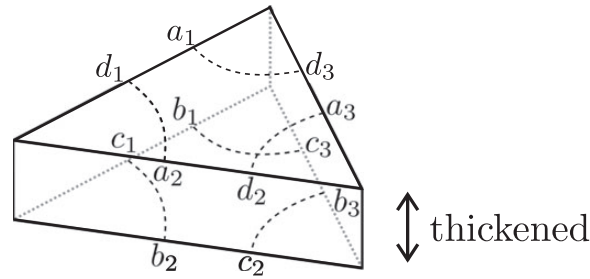


Fig. 6. Index lines on a triangle in the case of a matrix ring [1].

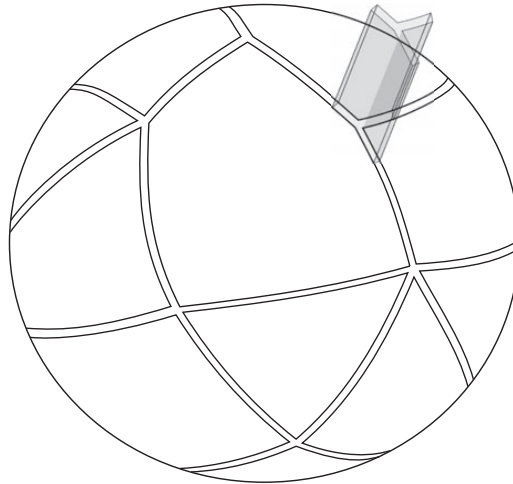


Fig. 7. A connected index network with double lines [1]. This represents a polygonal decomposition of a closed surface. Each polygon will be called an index polygon.

the action (2.13) can be rewritten in the form

$$\begin{aligned}
 S = & \frac{1}{2} \tilde{A}_{abcd} \tilde{B}^{abcd} - \frac{\lambda}{6n^3} \tilde{A}_{abcd} \tilde{A}_{befc} \tilde{A}_{eadf} \\
 & - \sum_{k \geq 2} \frac{n^2 \mu_k}{2k} \tilde{B}^{a_1 b_1 b_2 a_2} \tilde{B}^{a_2 b_2 b_3 a_3} \dots \tilde{B}^{a_k b_k b_1 a_1}.
 \end{aligned}
 \tag{2.17}$$

The way to contract the indices of \tilde{A} (or \tilde{B}) in the dual action (2.17) is the same as that of B (or A) in the original action (2.13). Thus, in the dual picture, the diagrams consist of polygons and 3-hinges, which are actually the dual diagrams to the original ones.

2.3. Restriction to tetrahedral decompositions

The diagrams generated in the model (2.13) consist of triangles whose edges are randomly glued together, and generally do not represent tetrahedral decompositions. However, one can define models such that the leading contributions in a large $N = n^2$ limit represent (only and all of the) tetrahedral decompositions. By denoting the defining associative algebra by $\mathcal{A}_{\text{grav}}$, this can be achieved by (i) taking $\mathcal{A}_{\text{grav}}$ to be $M_{n=3m}(\mathbb{R})$ with n a multiple of three, (ii) modifying the tensor

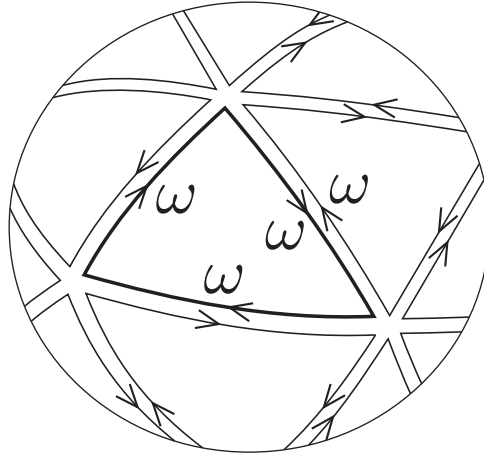


Fig. 8. A connected index network with double lines in the presence of a matrix ω [1].

$C^{a_1 b_1 c_1 d_1 a_2 b_2 c_2 d_2 a_3 b_3 c_3 d_3}$ from (2.15) to⁸

$$C_{\text{grav}}^{a_1 b_1 c_1 d_1 a_2 b_2 c_2 d_2 a_3 b_3 c_3 d_3} \equiv \frac{1}{n^3} \omega^{d_1 a_2} \omega^{d_2 a_3} \omega^{d_3 a_1} \omega^{b_3 c_2} \omega^{b_2 c_1} \omega^{b_1 c_3} \quad (2.18)$$

with a permutation matrix ω of the form

$$\omega \equiv \begin{pmatrix} 0 & 1_{n/3} & 0 \\ 0 & 0 & 1_{n/3} \\ 1_{n/3} & 0 & 0 \end{pmatrix}, \quad 1_m : m \times m \text{ unit matrix}, \quad (2.19)$$

and (iii) taking an appropriate limit for the parameters in the model [1].

In fact, with this modification, each index polygon with ℓ segments gives a factor $\text{tr } \omega^\ell$, which vanishes unless $\ell \equiv 0 \pmod{3}$ (see Fig. 8). Thus, the index function $\zeta(v) = \mathcal{I}_{g(v)}$ at vertex v takes a nonvanishing value ($=n^{2-2g(v)}$) only when the number of segments of every index polygon is a multiple of three. As proved in Ref. [1] in detail, the possible number of segments can be further reduced to three by taking the limit $n \rightarrow \infty$ with $n^2 \mu_k$ and n/λ being fixed, and there are left only such diagrams that represent tetrahedral decompositions.⁹

3. Introducing matter degrees of freedom

The above prescription to reduce the configurations to tetrahedral decompositions also works when $\mathcal{A}_{\text{grav}}$ is extended to a tensor product of the form $\mathcal{A} = \mathcal{A}_{\text{grav}} \otimes \mathcal{A}_{\text{mat}}$. Here, $\mathcal{A}_{\text{grav}}$ is again $M_{n=3m}(\mathbb{R})$, and \mathcal{A}_{mat} is another semisimple associative algebra to characterize the matter degrees of freedom. In fact, since the structure constants of \mathcal{A} are given by the product of the structure constants of $\mathcal{A}_{\text{grav}}$ and those of \mathcal{A}_{mat} , the index function $\mathcal{F}(\gamma)$ of each diagram γ is factorized to the product of the contributions from $\mathcal{A}_{\text{grav}}$ and \mathcal{A}_{mat} if we set the tensor C to take a factorized form $C = C_{\text{grav}} C_{\text{mat}}$:

$$\mathcal{F}(\gamma) \equiv \mathcal{F}(\gamma; \mathcal{A}) = \mathcal{F}(\gamma; \mathcal{A}_{\text{grav}}) \mathcal{F}(\gamma; \mathcal{A}_{\text{mat}}) \equiv \mathcal{F}_{\text{grav}}(\gamma) \mathcal{F}_{\text{mat}}(\gamma). \quad (3.1)$$

Then, by setting C_{grav} in the form (2.18) and by taking the limit $n \rightarrow \infty$ with $n^2 \mu_k$ and n/λ being fixed as in Sect. 2.3, the index function $\mathcal{F}(\gamma)$ vanishes unless γ represents a tetrahedral

⁸ This modification can be absorbed into a modification of the kinetic term by redefining A_{abcd} as $\omega^{d'a} A_{abcd} \omega^{bc'}$ \rightarrow $A_{d'c'd}$. One then can show that there still exists a duality between triangles and hinges.

⁹ The set of possible diagrams can be further reduced so as to represent 3D *manifolds* by introducing a parameter to control the number of vertices [1].

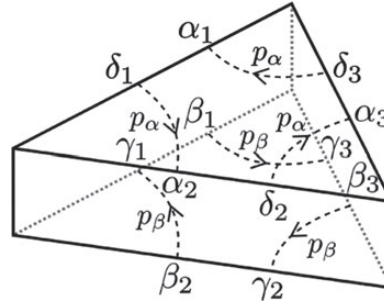


Fig. 9. A thickened triangle. The upper (lower) side has color α (β).

decomposition, and thus we can reduce the set of possible diagrams to tetrahedral decompositions independently of the choice of \mathcal{A}_{mat} .¹⁰ In this section, assuming that this reduction is already made, we show that a set of colors (representing matter degrees of freedom) can be assigned to simplices of arbitrary dimensions (tetrahedra, triangles, edges, and vertices) by choosing \mathcal{A}_{mat} and interaction terms appropriately.

Note that for $\mathcal{A} = \mathcal{A}_{\text{grav}} \otimes \mathcal{A}_{\text{mat}}$ the dynamical variables take the form $A_{abcd,ij}$ and $B^{abcd,ij}$, where (ab, cd) are matrix indices for $\mathcal{A}_{\text{grav}}$ and (i, j) are those for \mathcal{A}_{mat} . In the rest of the paper, we omit the indices a, b, \dots with respect to $\mathcal{A}_{\text{grav}}$ in order to simplify the expressions. We will denote the set of colors by \mathcal{J} and the number of elements by $|\mathcal{J}|$.

3.1. Coloring tetrahedra

We show that tetrahedra can be colored despite the fact that the action (2.2) does not have interaction terms corresponding to tetrahedra. We first set $\mathcal{A}_{\text{mat}} = M_{|\mathcal{J}|}(\mathbb{R}) = \bigoplus_{\alpha, \beta \in \mathcal{J}} \mathbb{R} e_{\alpha\beta}$ and let the interaction terms take the form¹¹

$$\begin{aligned}
 & - \sum_{\alpha, \beta \in \mathcal{J}} \frac{\lambda_{\alpha\beta}}{6|\mathcal{J}|^3} \sum_{\alpha_1, \dots, \delta_3 \in \mathcal{J}} A_{\alpha_1\beta_1\gamma_1\delta_1} A_{\alpha_2\beta_2\gamma_2\delta_2} A_{\alpha_3\beta_3\gamma_3\delta_3} \\
 & \times p_\alpha^{\delta_1\alpha_2} p_\alpha^{\delta_2\alpha_3} p_\alpha^{\delta_3\alpha_1} p_\beta^{\beta_3\gamma_2} p_\beta^{\beta_2\gamma_1} p_\beta^{\beta_1\gamma_3},
 \end{aligned} \tag{3.2}$$

where $\lambda_{\alpha\beta} = \lambda_{\beta\alpha}$, and p_α is the projection matrix to the α th component:

$$p_\alpha^{\alpha_1\alpha_2} = \delta_\alpha^{\alpha_1} \delta_\alpha^{\alpha_2}. \tag{3.3}$$

The interaction terms can be expressed by thickened triangles as in Fig. 9, where the projection matrices p_α and p_β are inserted into the index lines such that each side of the triangle has its own color. Thus, each index triangle at a corner of a tetrahedron gives a factor of the form $\text{tr}(p_{\alpha_1} p_{\alpha_2} p_{\alpha_3})$ if there meet three triangles with colors $\alpha_1, \alpha_2, \alpha_3$ at the corner (see Fig. 10). Since there are four

¹⁰ Note that the introduction of matter degrees of freedom may further reduce the set of possible diagrams because $\mathcal{F}_{\text{mat}}(\gamma)$ may vanish for a subset of simplicial decompositions.

¹¹ Recall that we are only looking at the matter part. Actually, the variable A has extra indices of $\mathcal{A}_{\text{grav}} = M_{n=3m}(\mathbb{R})$ as $A_{abcd, \alpha\beta\gamma\delta}$, and the interaction terms (3.2) have extra factors (2.18).

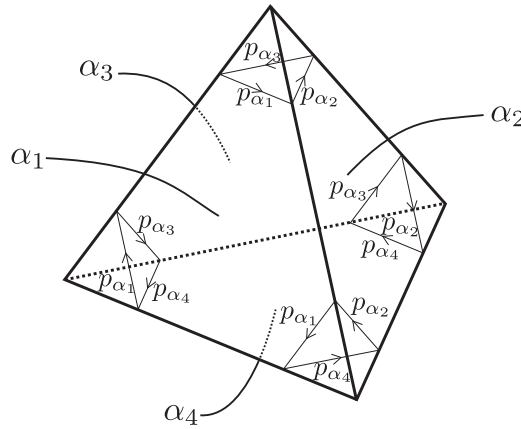


Fig. 10. Index triangles inside a tetrahedron with triangles colored as in (3.2).

corners in a tetrahedron, the tetrahedron illustrated in Fig. 10 gives the factor

$$\begin{aligned} & \text{tr}(p_{\alpha_1} p_{\alpha_2} p_{\alpha_3}) \text{tr}(p_{\alpha_2} p_{\alpha_1} p_{\alpha_4}) \text{tr}(p_{\alpha_1} p_{\alpha_3} p_{\alpha_4}) \text{tr}(p_{\alpha_3} p_{\alpha_2} p_{\alpha_4}) \\ &= \begin{cases} 1 & (\alpha_1 = \alpha_2 = \alpha_3 = \alpha_4) \\ 0 & (\text{otherwise}) \end{cases}. \end{aligned} \tag{3.4}$$

This means that the index function $\mathcal{F}(\gamma)$ can take nonvanishing values only when four index triangles of each tetrahedron have the same color (say, α), which enables us to say that the tetrahedron has a definite color α . We thus succeed in coloring tetrahedra in γ . The parameters $\lambda_{\alpha\beta}$ in (3.2) represent the coupling constants of local interactions among matter degrees of freedom on tetrahedra, because $\lambda_{\alpha\beta}$ appears in $\mathcal{F}(\gamma)$ when the corresponding triangle is shared by neighboring tetrahedra of colors α and β .

If we take the set of colors to be $\mathcal{J} = \mathbb{R}^D = \{\mathbf{x}\}$ and let the coupling constants $\lambda_{\mathbf{x},\mathbf{y}}$ ($\mathbf{x}, \mathbf{y} \in \mathbb{R}^D$) take nonvanishing values only around \mathbf{y} as a function of \mathbf{x} , then \mathbf{x} can be interpreted as the target space coordinates of a tetrahedron in \mathbb{R}^D . Since neighboring tetrahedra are locally connected in \mathbb{R}^D , the model can describe the dynamics of membranes in \mathbb{R}^D . Instead, if we take \mathcal{J} to be a finite set with $|\mathcal{J}| = q$, then the model can describe a q -state spin system on random volumes. In particular, if we consider the case $q = 2$ (with colors $\alpha = \pm$), then the model represents 3D quantum gravity coupled to the Ising model. The system is ferromagnetic when $\lambda_{++} \geq \lambda_{+-}$ and $\lambda_{--} \geq \lambda_{+-}$. If the global \mathbb{Z}_2 symmetry ($+ \leftrightarrow -$) is explicitly broken by setting $\lambda_{++} \neq \lambda_{--}$, then the model describes a system in the presence of an external magnetic field. With generic q , we can construct q -state Potts models or RSOS models [26] on random volumes by appropriately choosing $\lambda_{\alpha\beta}$.

3.2. Coloring triangles

Triangles can be colored by making an argument similar to the one in Sect. 3.1. We set $\mathcal{A}_{\text{mat}} = M_s(\mathbb{R}) = \bigoplus_{\alpha,\beta=1}^s \mathbb{R}e_{\alpha\beta}$,¹² and let the interaction terms take the form

$$- \sum_{\mu \in \mathcal{J}} \frac{\lambda_\mu}{6s^2} A_{\alpha_1\beta_1\gamma_1\delta_1} A_{\alpha_2\beta_2\gamma_2\delta_2} A_{\alpha_3\beta_3\gamma_3\delta_3} u_\mu^{\delta_1\alpha_2} u_\mu^{\delta_2\alpha_3} u_\mu^{\delta_3\alpha_1} u_\mu^{\beta_3\gamma_2} u_\mu^{\beta_2\gamma_1} u_\mu^{\beta_1\gamma_3}. \tag{3.5}$$

¹² The linear dimension s can be set to any value as long as the coupling constants (3.6) take the desired forms.

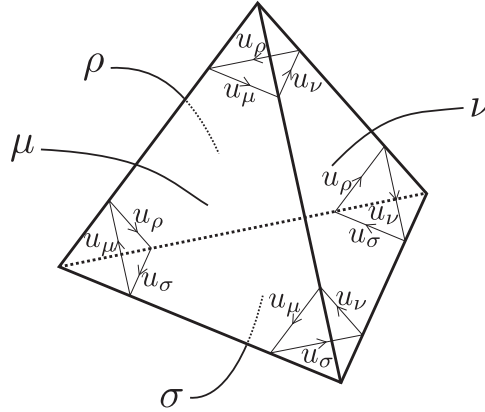


Fig. 11. Index triangles inside a tetrahedron formed by colored triangles.

The model with (3.5) generates diagrams where a color μ ($\mu \in \mathcal{J}$) is assigned to each triangle. If three triangles (with colors μ, ν, ρ) meet at a corner of a tetrahedron to construct an index triangle, the index function gets the factor $\text{tr}(u_\mu u_\nu u_\rho)$. Then, the tetrahedron illustrated in Fig. 11 gives a factor of the form

$$\text{tr}(u_\mu u_\nu u_\rho) \text{tr}(u_\nu u_\mu u_\sigma) \text{tr}(u_\mu u_\rho u_\sigma) \text{tr}(u_\rho u_\nu u_\sigma). \quad (3.6)$$

Such factors behave as the coupling constants of local interactions among matter degrees of freedom located on triangles.

There is another prescription to assign colors to triangles. We introduce $|\mathcal{J}|$ copies of variables A and B (denoted by $A^{(r)}$ and $B^{(r)}$ ($r = 1, \dots, |\mathcal{J}|$)), and let the action take the form

$$S = \sum_{r \in \mathcal{J}} \frac{1}{2} A_{ij}^{(r)} B_{(r)}^{ij} - \sum_{r \in \mathcal{J}} \frac{\lambda_r}{6} A_{ij}^{(r)} A_{kl}^{(r)} A_{mn}^{(r)} g^{jk} g^{lm} g^{ni} - \sum_{r_1, \dots, r_k \in \mathcal{J}} \sum_{k \geq 2} \frac{\mu_k^{r_1, \dots, r_k}}{2k} B_{(r_1)}^{i_1 j_1} \dots B_{(r_k)}^{i_k j_k} y_{i_1, \dots, i_k} y_{j_k, \dots, j_1}. \quad (3.7)$$

Then, this model also generates tetrahedral decompositions with colored triangles. The index function $\mathcal{F}(\gamma)$ of the model (3.7) gets the factor $\mu_k^{r_1, \dots, r_k}$ from a k -hinge shared by k triangles with colors r_1, \dots, r_k , and thus has a form different from (3.6). Therefore, although matter degrees of freedom are assigned to triangles in both (3.5) and (3.7), they give different local interactions (at least apparently).

3.3. Coloring edges

There are two prescriptions to assign colors to edges, as is the case in coloring triangles.

As in the first prescription in Sect. 3.2, we take $\mathcal{A}_{\text{mat}} = M_s(\mathbb{R}) = \bigoplus_{\alpha, \beta=1}^s \mathbb{R} e_{\alpha\beta}$. We now let the interaction terms corresponding to hinges take the form

$$- \sum_{m \in \mathcal{J}} \sum_{k \geq 2} \frac{s^2 \mu_k^m}{2k} B^{\alpha_1 \beta_1 \gamma_1 \delta_1} \dots B^{\alpha_k \beta_k \gamma_k \delta_k} u_{\beta_1 \alpha_2}^m \dots u_{\beta_k \alpha_1}^m u_{\gamma_1 \delta_2}^m \dots u_{\gamma_k \delta_1}^m. \quad (3.8)$$

This generates diagrams where each edge has a color m ($m \in \mathcal{J}$), and each index triangle gives the factor $\text{tr}(u^{m_1} u^{m_2} u^{m_3})$ depending on the colors of the edges. They give the coupling constants of local interactions among matter degrees of freedom located on edges.

Another prescription to assign colors to edges can be given by modifying the action (2.2) to the form

$$S = \sum_{r \in \mathcal{J}} \frac{1}{2} A_{ij}^{(r)} B_{(r)}^{ij} - \sum_{r_1, r_2, r_3 \in \mathcal{J}} \frac{\lambda_{r_1 r_2 r_3}}{6} A_{ij}^{(r_1)} A_{kl}^{(r_2)} A_{mn}^{(r_3)} g^{jk} g^{lm} g^{ni} - \sum_{r \in \mathcal{J}} \sum_{k \geq 2} \frac{\mu_k}{2k} B_{(r)}^{i_1 j_1} \cdots B_{(r)}^{i_k j_k} y_{i_1, \dots, i_k} y_{j_k, \dots, j_1}. \tag{3.9}$$

Each triangle gives the factor $\lambda_{r_1 r_2 r_3}$ if three hinges (with colors r_1, r_2, r_3) meet there.

3.4. Coloring vertices

Vertices can also be colored despite the fact that the action (2.2) does not have interaction terms corresponding to vertices.

We first set the matter associative algebra to be $\mathcal{A}_{\text{mat}} = \mathcal{A}_{\text{mat}}^{(1)} \oplus \cdots \oplus \mathcal{A}_{\text{mat}}^{(|\mathcal{J}|)}$, and let the interaction terms corresponding to hinges take the form

$$- \sum_{\alpha, \beta \in \mathcal{J}} \sum_{k \geq 2} \frac{\mu_k^{\alpha\beta}}{2k} B^{i_1 j_1} \cdots B^{i_k j_k} y_{i_1, \dots, i_k}^{(\alpha)} y_{j_k, \dots, j_1}^{(\beta)}. \tag{3.10}$$

Here $y_{i_1, \dots, i_k}^{(\alpha)}$ are the coupling constants constructed from the structure constants $y_{ij}^{(\alpha)k}$ of $\mathcal{A}_{\text{mat}}^{(\alpha)}$ and take nonvanishing values only when all the indices i_1, \dots, i_k belong to $\mathcal{A}_{\text{mat}}^{(\alpha)}$. Accordingly, all the junctions in the same connected index network should have the same color α in order for the index function $\mathcal{F}(\gamma)$ to take nonvanishing values. Thus, we can assign a color to the index network of each vertex in diagram γ , and can say that the model generates diagrams with colored vertices. The matter degrees of freedom located on vertices have local interactions, and having two neighboring vertices with colors α and β (connected by a hinge) gives the factor $\mu_k^{\alpha\beta}$ to $\mathcal{F}(\gamma)$.

The above coloring of vertices can also be realized by setting $\mathcal{A}_{\text{mat}} = M_{|\mathcal{J}|}(\mathbb{R})$ and letting the interaction terms corresponding to hinges take the form

$$- \sum_{\alpha, \beta \in \mathcal{J}} \sum_{k \geq 2} \frac{|\mathcal{J}|^2 \mu_k^{\alpha\beta}}{2k} B^{\alpha_1 \beta_1 \gamma_1 \delta_1} \cdots B^{\alpha_k \beta_k \gamma_k \delta_k} p_{\beta_1 \alpha_2}^\alpha \cdots p_{\beta_k \alpha_1}^\beta p_{\gamma_1 \delta_2}^\beta \cdots p_{\gamma_k \delta_1}^\beta, \tag{3.11}$$

where p^α is the projection matrix to the α th component (the same as the one given in (3.3)). It is easy to see that this model is dual to the model with (3.2) through the duality transformation (2.16). That is, the action with the interaction term (3.11) can be regarded as a q -state system on the dual lattice of γ ($q = |\mathcal{J}|$).

We thus conclude that matter degrees of freedom can be introduced to triangle–hinge models such that they live on simplices of any dimensions and interact with themselves locally.

4. Relations to colored tensor models

We can further construct various kinds of models by combining several prescriptions explained in the previous section. For example, we show in this section that 3D colored tensor models [29] can be realized as triangle–hinge models by coloring tetrahedra, triangles, and edges *at one time*.

4.1. Feynman rules of colored tensor models

We first review the Feynman rules of 3D colored tensor models (see, e.g., Ref. [29] for a review). The dynamical variables of colored tensor models are given by a pair of rank-three tensors ϕ_{LJK}^μ and $\bar{\phi}_{LJK}^\mu$

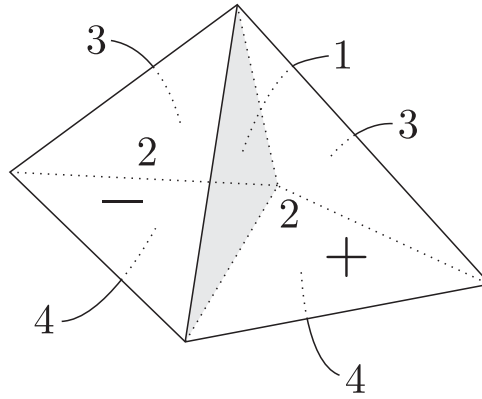


Fig. 12. Part of a Feynman diagram in colored tensor models. There are two tetrahedra, one corresponding to an interaction vertex proportional to κ and the other to $\bar{\kappa}$. The two adjacent tetrahedra have opposite orientations.

with no symmetry properties under permutations of the subscripts I, J, K . The tensors represent two kinds of colored triangles, where $\{I\}$ is the set of indices assigned to edges, and $\{\mu\} = \{1, 2, 3, 4\}$ are the colors assigned to triangles.¹³ The action takes the form

$$S = \sum_{\mu=1}^4 \phi_{IJK}^{\mu} \bar{\phi}_{IJK}^{\mu} + \kappa \phi_{IJK}^1 \phi_{KML}^2 \phi_{MKN}^3 \phi_{LNI}^4 + \bar{\kappa} \bar{\phi}_{IJK}^1 \bar{\phi}_{KML}^2 \bar{\phi}_{MKN}^3 \bar{\phi}_{LNI}^4. \quad (4.1)$$

Looking at the way of contraction of indices I , one easily sees that this action generates Feynman diagrams where the interaction vertices can be identified with tetrahedra that are glued at their faces through the propagator. Since there are two types of interaction terms $\kappa \phi^4$ and $\bar{\kappa} \bar{\phi}^4$, the set of tetrahedra can be decomposed to two different classes, which we label with $\alpha = \pm$, respectively. We assign four different colors $\mu = 1, \dots, 4$ to four triangles of each tetrahedron. This coloring of triangles naturally introduces the coloring of six edges in a tetrahedron, and we assign color $(\mu\nu) = (\nu\mu)$ to an edge if the edge is shared by two triangles with colors μ and ν ($\mu \neq \nu$). Since the tensors ϕ_{IJK}^{μ} and $\bar{\phi}_{IJK}^{\mu}$ have no permutation symmetry with respect to the subscripts, two tetrahedra can be glued at their faces only when two triangles to be identified have the same color μ and two edges to be identified have the same color $(\mu\nu)$, as in Fig. 12. We say that the tetrahedron has positive (or negative) orientation if triangles 1, 2, 3 are located clockwise (or counterclockwise) when seen from triangle 4 (see Fig. 12). Since the kinetic term has the form $\phi \bar{\phi}$ (not including ϕ^2 or $\bar{\phi}^2$), two adjacent tetrahedra must have different orientations.

The Feynman rules for colored tensor models (4.1) can thus be summarized as follows:

1. Interaction vertices are represented by two types (orientations) of tetrahedra, $\alpha = \pm$, and any two adjacent tetrahedra have different types.
2. Four different colors $\mu = 1, \dots, 4$ are assigned to four triangles of each tetrahedron, such that the assignment agrees with the orientation of the tetrahedron when $\alpha = +$, while it is opposite when $\alpha = -$.
3. Two tetrahedra are glued at their faces in such a way that two triangles to be identified have the same color μ and two edges to be identified have the same color $(\mu\nu)$.

¹³ In the original Boulatov model [13] the index I runs over the elements of group manifold $SU(2)$.

4.2. Realization of colored tensor models as triangle–hinge models

The above Feynman rules for 3D colored tensor models can be reproduced from triangle–hinge models by coloring tetrahedra, triangles, and edges at one time. To see this, we set the matter associative algebra \mathcal{A}_{mat} to be a matrix ring $M_{2s}(\mathbb{R})$ and let the action take the form

$$\begin{aligned}
 S = & \sum_{(\mu\nu)} \frac{1}{2} A_{\alpha\beta\gamma\delta}^{(\mu\nu)} B_{(\mu\nu)}^{\alpha\beta\gamma\delta} - \frac{\lambda}{6(2s)^3} \sum_{\mu=1}^4 \frac{1}{6} \sum_{\substack{v,\rho,\sigma=1 \\ (\mu\nu\rho\sigma): \text{ all different}}}^4 A_{\alpha_1\beta_1\gamma_1\delta_1}^{(\mu\nu)} A_{\alpha_2\beta_2\gamma_2\delta_2}^{(\mu\rho)} A_{\alpha_3\beta_3\gamma_3\delta_3}^{(\mu\sigma)} \\
 & \times \left(u_{+\mu}^{\delta_1\alpha_2} u_{+\mu}^{\delta_2\alpha_3} u_{+\mu}^{\delta_3\alpha_1} u_{-\mu}^{\beta_3\gamma_2} u_{-\mu}^{\beta_2\gamma_1} u_{-\mu}^{\beta_1\gamma_3} + u_{-\mu}^{\delta_1\alpha_2} u_{-\mu}^{\delta_2\alpha_3} u_{-\mu}^{\delta_3\alpha_1} u_{+\mu}^{\beta_3\gamma_2} u_{+\mu}^{\beta_2\gamma_1} u_{+\mu}^{\beta_1\gamma_3} \right) \\
 & - \sum_{k \geq 2} \frac{n^2 \mu_k}{2k} \sum_{(\mu\nu)} B_{(\mu\nu)}^{\alpha_1\alpha_2\beta_2\beta_1} B_{(\mu\nu)}^{\alpha_2\alpha_3\beta_3\beta_2} \dots B_{(\mu\nu)}^{\alpha_k\alpha_1\beta_1\beta_k}. \tag{4.2}
 \end{aligned}$$

Here, the indices $(\mu\nu) = (v\mu)$ ($\mu, v = 1, \dots, 4; \mu \neq v$) stand for the colors assigned to edges, the sum $\sum_{(\mu\nu)}$ is taken over all different colors of edges, and we have again neglected the gravity part, which ensures that the resulting Feynman diagrams form a set of tetrahedra (see footnote 11). We further assume the matrices $u_{\pm\mu}$ to have the form

$$u_{+\mu} = \begin{pmatrix} u_\mu & 0 \\ 0 & 0 \end{pmatrix}, \quad u_{-\mu} = \begin{pmatrix} 0 & 0 \\ 0 & (u_\mu)^T \end{pmatrix}. \tag{4.3}$$

Here $s \times s$ matrices u_μ are chosen such that they satisfy¹⁴

$$\text{tr}(u_\mu u_\nu u_\rho) \text{tr}(u_\nu u_\mu u_\sigma) \text{tr}(u_\mu u_\rho u_\sigma) \text{tr}(u_\rho u_\nu u_\sigma) = \begin{cases} 1 & (\epsilon_{\mu\nu\rho\sigma} = +1) \\ 0 & (\text{otherwise}) \end{cases}, \tag{4.4}$$

where $\epsilon_{\mu\nu\rho\sigma}$ is the totally antisymmetric tensor with $\epsilon_{1234} = 1$. The interaction vertices corresponding to triangles can be expressed by thickened triangles as in Fig. 13. Note that we make colorings for simplices of three different dimensions (tetrahedra, triangles, and edges), which are described in Sects. 3.1, 3.2, and 3.3, respectively. In fact, each tetrahedron has a type (orientation) $\alpha = \pm$, each triangle has a color $\mu = 1, \dots, 4$, and each edge has a color $(\mu\nu) = (v\mu)$ ($\mu \neq v$). The interaction terms corresponding to triangles indicate that the three edges of a triangle of color μ have different colors $(\mu\nu), (\mu\rho), (\mu\sigma)$. Note that we particularly set $\lambda_{\alpha\beta}$ as $\lambda_{++} = \lambda_{--} = 0$ (and $\lambda_{+-} = \lambda_{-+} = \lambda$), so that any two adjacent tetrahedra have different types. As can be seen from (3.6), a tetrahedron of type $\alpha = +$ (or $\alpha = -$) gives the factor

$$\text{tr}(u_{\alpha\mu} u_{\alpha\nu} u_{\alpha\rho}) \text{tr}(u_{\alpha\nu} u_{\alpha\mu} u_{\alpha\sigma}) \text{tr}(u_{\alpha\mu} u_{\alpha\rho} u_{\alpha\sigma}) \text{tr}(u_{\alpha\rho} u_{\alpha\nu} u_{\alpha\sigma}) \quad (\alpha = \pm), \tag{4.5}$$

which takes a nonvanishing value ($= 1$) only when the four colors μ, ν, ρ, σ are all different and correspond to the positive (or negative) orientation. Thus, a tetrahedron in a nonvanishing Feynman

¹⁴ For example, one can take the following 6×6 matrices:

$$\begin{aligned}
 u_1 = 2^{-\frac{1}{2}} \begin{pmatrix} 0 & \sigma_1 & 0 \\ 0 & 0 & \sigma_1 \\ 0 & 0 & 0 \end{pmatrix}, \quad u_2 = 2^{-\frac{2}{3}} \begin{pmatrix} 0 & 0 & 0 \\ 0 & 0 & -i\sigma_2 \\ -i\sigma_2 & 0 & 0 \end{pmatrix}, \\
 u_3 = 2^{-\frac{1}{2}} \begin{pmatrix} 0 & \sigma_3 & 0 \\ 0 & 0 & 0 \\ \sigma_3 & 0 & 0 \end{pmatrix}, \quad u_4 = 2^{\frac{1}{3}} \begin{pmatrix} 1 & i\sigma_2 & 0 \\ 0 & 1 & -\sigma_3 \\ -\sigma_1 & 0 & 1 \end{pmatrix},
 \end{aligned}$$

where σ_i ($i = 1, 2, 3$) are the Pauli matrices.

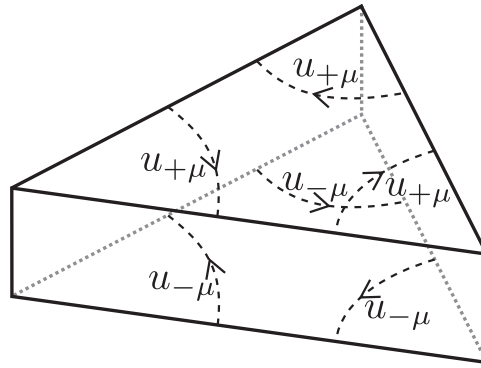


Fig. 13. A thickened triangle vertex coming from the action (4.2), which realizes colored tensor models.

diagram has a positive orientation when its color is $\alpha = +$ and a negative orientation when $\alpha = -$. Furthermore, if two triangles sharing an edge of color $(\mu\nu)$ ($\mu \neq \nu$) belong to the same tetrahedron, then one of the two triangles has color μ and the other has color ν . In fact, any triangle connected to a hinge of color $(\mu\nu)$ must have color μ or ν , but two triangles sharing the edge $(\mu\nu)$ must have different colors if they belong to the same tetrahedron.

Therefore, the Feynman diagrams generated by the action (4.2) consist of tetrahedra where two adjacent tetrahedra have different orientations $\alpha = \pm$, and four triangles in each tetrahedron have different colors $\mu = 1, \dots, 4$ so as to be consistent with the orientation of the tetrahedron. Furthermore, the coloring of each edge does not depend on the choice of a tetrahedron including the edge, which leads us to the interpretation that two tetrahedra are glued at their faces such that the edges to be identified have the same color. We thus conclude that the Feynman diagrams obtained from the action (4.2) obey the same Feynman rules obtained from the action (4.1) of 3D colored tensor models.

5. Conclusion

In this paper, we give a general prescription to introduce matter degrees of freedom to triangle–hinge models. This is achieved by setting the defining associative algebra \mathcal{A} to be a tensor product of the form $\mathcal{A}_{\text{grav}} \otimes \mathcal{A}_{\text{mat}}$ and by modifying the interaction terms appropriately. The matter fields thus obtained have local interactions, since a colored tetrahedron can only interact with the neighbors. We can assign colors not only to tetrahedra but also to simplices of arbitrary dimensions. We further show that there exists a duality between matter fields on a tetrahedral lattice and those on its dual lattice, which can be realized by applying the duality transformation (2.16), which interchanges the roles of triangles and hinges.

When we take the set of colors to be \mathbb{R}^D and assign colors to tetrahedra as in (3.2), the matter fields represent the target space coordinates of membranes in D dimensions. By taking different sets of colors, we can also construct various spin systems on random volumes, including the Ising model, q -state Potts models, and RSOS models.

A wider class of models can be further obtained as triangle–hinge models by coloring lower-dimensional simplices as well as tetrahedra. For example, 3D colored tensor models can be obtained by coloring tetrahedra, triangles, and edges at one time. This is shown in Sect. 4.2 by explicitly demonstrating that the same Feynman rules are obtained.

It should be interesting to investigate the critical behaviors of triangle–hinge models with matter fields. In particular, it is important to study the case when matter fields correspond to the target space coordinates of embedded membranes. It would also be interesting to investigate if there is any obstacle in introducing matter fields like the “ $c = 1$ barrier” for matter fields on random surfaces. Introduction of supersymmetry to triangle–hinge models is another interesting problem. Studies in these directions are now in progress and will be communicated elsewhere.

Acknowledgements

The authors thank Naoki Sasakura for useful discussions. M.F. is supported by MEXT (Grant No. 23540304). S.S. is supported by the JSPS fellowship.

Funding

Open Access funding: SCOAP³.

References

- [1] M. Fukuma, S. Sugishita, and N. Umeda, *J. High Energy Phys.* **1507**, 088 (2015) [[arXiv:1503.08812](#) [hep-th]] [[Search INSPIRE](#)].
- [2] C. M. Hull and P. K. Townsend, *Nucl. Phys. B* **438**, 109 (1995) [[arXiv:hep-th/9410167](#)] [[Search INSPIRE](#)].
- [3] P. K. Townsend, *Phys. Lett. B* **350**, 184 (1995) [[arXiv:hep-th/9501068](#)] [[Search INSPIRE](#)].
- [4] E. Witten, *Nucl. Phys. B* **443**, 85 (1995) [[arXiv:hep-th/9503124](#)] [[Search INSPIRE](#)].
- [5] J. H. Schwarz, *Phys. Lett. B* **367**, 97 (1996) [[arXiv:hep-th/9510086](#)] [[Search INSPIRE](#)].
- [6] P. Hořava and E. Witten, *Nucl. Phys. B* **460**, 506 (1996) [[arXiv:hep-th/9510209](#)] [[Search INSPIRE](#)].
- [7] A. M. Polyakov, *Gauge Fields and Strings: Contemporary Concepts in Physics* (CRC press, USA, 1987), Vol. 3.
- [8] P. Di Francesco, P. H. Ginsparg, and J. Zinn-Justin, *Phys. Rept.* **254**, 1 (1995) [[arXiv:hep-th/9306153](#)] [[Search INSPIRE](#)].
- [9] S. W. Chung, M. Fukuma, and A. D. Shapere, *Int. J. Mod. Phys. A* **9**, 1305 (1994) [[arXiv:hep-th/9305080](#)] [[Search INSPIRE](#)].
- [10] J. Ambjørn, B. Durhuus, and T. Jonsson, *Mod. Phys. Lett. A* **6**, 1133 (1991).
- [11] N. Sasakura, *Mod. Phys. Lett. A* **6**, 2613 (1991).
- [12] M. Gross, *Nucl. Phys. B - Proc. Suppl.* **25**, 144 (1992).
- [13] D. V. Boulatov, *Mod. Phys. Lett. A* **7**, 1629 (1992) [[arXiv:hep-th/9202074](#)] [[Search INSPIRE](#)].
- [14] L. Freidel, *Int. J. Theor. Phys.* **44**, 1769 (2005) [[arXiv:hep-th/0505016](#)] [[Search INSPIRE](#)].
- [15] N. Sasakura, *Int. J. Mod. Phys. A* **27**, 1250020 (2012) [[arXiv:1111.2790](#) [hep-th]] [[Search INSPIRE](#)].
- [16] N. Sasakura, *Int. J. Mod. Phys. A* **27**, 1250096 (2012) [[arXiv:1203.0421](#) [hep-th]] [[Search INSPIRE](#)].
- [17] N. Sasakura, *Int. J. Mod. Phys. A* **28**, 1350030 (2013) [[arXiv:1302.1656](#) [hep-th]] [[Search INSPIRE](#)].
- [18] N. Sasakura, *Int. J. Mod. Phys. A* **28**, 1350111 (2013) [[arXiv:1305.6389](#) [hep-th]] [[Search INSPIRE](#)].
- [19] N. Sasakura and Y. Sato, *Phys. Lett. B* **732**, 32 (2014) [[arXiv:1401.2062](#) [hep-th]] [[Search INSPIRE](#)].
- [20] N. Sasakura and Y. Sato, *J. High Energy Phys.* **1510**, 109 (2015) [[arXiv:1506.04872](#) [hep-th]] [[Search INSPIRE](#)].
- [21] N. Sasakura and Y. Sato, *Prog. Theor. Exp. Phys.* **2014**, 053B03 (2014) [[arXiv:1401.7806](#) [hep-th]] [[Search INSPIRE](#)].
- [22] G. Narain, N. Sasakura, and Y. Sato, *J. High Energy Phys.* **1501**, 010 (2015) [[arXiv:1410.2683](#) [hep-th]] [[Search INSPIRE](#)].
- [23] N. Sasakura and Y. Sato, *Prog. Theor. Exp. Phys.* **2015**, 043B09 (2015) [[arXiv:1501.05078](#) [hep-th]] [[Search INSPIRE](#)].
- [24] G. Narain and N. Sasakura, *Prog. Theor. Exp. Phys.* **2015**, 123A05 (2015) [[arXiv:1509.01432](#) [hep-th]] [[Search INSPIRE](#)].
- [25] H. Chen, N. Sasakura, and Y. Sato, [[arXiv:1601.04232](#) [hep-th]] [[Search INSPIRE](#)].
- [26] C. Itzykson and J. M. Drouffe, *Statistical Field Theory, Vol. 1: From Brownian Motion To Renormalization and Lattice Gauge Theory* (Cambridge University Press, Cambridge, UK, 1989).

- [27] R. Gurau, Commun. Math. Phys. **304**, 69 (2011) [[arXiv:0907.2582](#) [hep-th]] [[Search INSPIRE](#)].
- [28] R. Gurau, Classical Quantum Gravity **27**, 235023 (2010) [[arXiv:1006.0714](#) [hep-th]] [[Search INSPIRE](#)].
- [29] R. Gurau and J. P. Ryan, SIGMA **8**, 020 (2012) [[arXiv:1109.4812](#) [hep-th]] [[Search INSPIRE](#)].
- [30] M. Fukuma, S. Hosono, and H. Kawai, Commun. Math. Phys. **161**, 157 (1994) [[arXiv:hep-th/9212154](#)] [[Search INSPIRE](#)].